

Fault-Tolerant Trajectory Tracking Control of a Quadrotor Helicopter Using Gain-Scheduled PID and Model Reference Adaptive Control

Iman Sadeghzadeh¹, Ankit Mehta², Youmin Zhang^{3*} and Camille-Alain Rabbath⁴

^{1,2,3}Concordia University, Montreal, Quebec, H3G 1M8, Canada

i_sade@encs.concordia.ca
an_mehta@encs.concordia.ca
**ymzhang@encs.concordia.ca*

⁴Defence Research and Development Canada, Valcartier, G3J 1X5 Quebec, Canada

Camille-Alain.Rabbath@drdc-rddc.gc.ca

ABSTRACT

Based on two successfully and widely used control techniques in many industrial applications under normal (fault-free) operation conditions, the Gain-Scheduled Proportional-Integral-Derivative (GS-PID) control and Model Reference Adaptive Control (MRAC) strategies have been extended, implemented, and experimentally tested on a quadrotor helicopter Unmanned Aerial Vehicle (UAV) test-bed available at Concordia University, for the purpose of investigation of these two typical and different control techniques as two useful Fault-Tolerant Control (FTC) approaches. Controllers are designed and implemented in order to track the desired trajectory of the helicopter in both normal and faulty scenarios of the flight. A Linear Quadratic Regulator (LQR) with integral action controller is also used to control the pitch and roll motion of the quadrotor helicopter. Square trajectory, together with specified autonomous and safe taking-off and landing path, is considered as the testing trajectory and the experimental flight testing results with both GS-PID and MRAC are presented and compared with tracking performance under partial loss of control power due to fault/damage in the propeller of the quadrotor UAV. The performance of both controllers showed to be good. Although GS-PID is easier for development and implementation, MRAC showed to be more robust to faults and noises, and is friendly to be applied to the quadrotor UAV.

1. INTRODUCTION

Safety, reliability and acceptable level of performance of dynamic control systems are key requirements in control systems not only in normal operation conditions but also in the presence of partial fault or failure in the components of the controlled system. Hence, the role of Fault-Tolerant

Control Systems (FTCS) is revealed evidently (Zhang & Jiang, 2008). In fact, when a fault occurs in a system, it suddenly starts to behave in an unanticipated manner with the originally designed baseline controller(s) under normal conditions. Therefore, fault-tolerant controller must be designed, implemented and executed on-line and in real-time to be able to handle the fault and to guarantee system stability and acceptable performance even in the presence of faults in actuators, sensors and other system components.

There are different techniques to handle such faults. As one of adaptive control techniques, Model Reference Adaptive Control (MRAC) is one of the recently widely investigated techniques for handling different fault situations with different types of aircraft applications as demonstrated in the recent AIAA Guidance, Navigation, and Control Conference (Bierling, Hocht, & Holzapfel, 2010; Crespo, Matsutani, & Annaswamy, 2010; Dydek & Annaswamy, 2010; Gadiant, Levin, & Lavretsky, 2010; Gregory, Gadiant, & Lavretsky, 2011; Guo & Tao, 2010; Jourdan et al, 2010; Lemon, Steck, & Hinson, 2010; Levin, 2010; Stepanyan, Campbell, & Krishnakumar, 2010; Whitehead & Bieniawski, 2010). MRAC is concerned with forcing the dynamic response of the controlled system to asymptotically approach that of reference system, despite parametric uncertainties in the plant. In fact, adaptive control is originally a control technique which bases on a concept that controllers must adapt to a controlled system with parameters which vary slowly, or are initially uncertain. For example, as an aircraft flies, its mass will slowly decrease as a result of fuel consumption. To maintain good control performance under such varying conditions, an adaptive control law is needed to adapt itself to such changing conditions. Based on its adaptive and self-tuning capability in the presence of system parameters changes, including such changes due to faults/damages, there are a trend for

¹Ph.D. Student, Department of Mechanical and Industrial Engineering

²M.Eng Student, Department of Mechanical and Industrial Engineering

³Associate Professor, Department of Mechanical and Industrial Engineering, Corresponding Author

⁴Defense Scientist, DRDC - Valcartier, 2459 Pie-XI Blvd. North

investigating the potential application of MRAC for fault-tolerant control of aircraft and UAVs recently. However, there is no published research result for using MRAC to fault-tolerant tracking control of quadrotor helicopter UAVs, which in fact motivated the work to be presented in this paper.

On the other hand, Proportional-Integral-Derivative (PID) controllers are the most widely used controllers in industry due to its unique feature without the need of a mathematical model of the controlled system for controller design, implementation and real-time execution. PID controllers are reliable and easy to use and can be used for linear and non-linear systems with certain level of robustness to the uncertainties and disturbances. Although one single PID controller can handle even wide range of system nonlinearities, to handle the possible fault conditions of a quadrotor helicopter UAV, multiple PIDs need to be designed to control the quadrotor helicopter UAV with acceptable performance under both normal and different faulty flight conditions. For such a purpose, the Gain-Scheduled PID (GS-PID) control strategy was initially proposed to be applied to a quadrotor helicopter UAV for achieving fault-tolerant control by Bani Milhim, Zhang, & Rabbath (2010). However, such a work was based only on simulation due to the lack of a physical UAV test-bed at that time. At the same conference of the 2010 AIAA Infotech@Aerospace, Johnson, Chowdhary, & Kimbrell (2010) also investigated a GS-PID scheme to their GTech Twinstar fixed-wing research vehicle.

In view of the advantages and potentials of using GS-PID for handling fault conditions, it motivated us to further investigate and most importantly to experimentally test the GS-PID controller in a physical quadrotor UAV test-bed at the Networked Autonomous Vehicles Lab of Concordia University, for fault-tolerant three-dimensional trajectory tracking control, instead of implementing the GS-PID only for one-dimensional height hold flight conditions. In this paper, GS-PID has been implemented for different sections of the entire flight envelope by properly tuning the PID controller gains for both normal and fault conditions. A Fault Detection and Diagnosis (FDD) scheme is assumed to be available for providing the time and the magnitude of the fault during the flight. Based on the decision of the FDD scheme about the fault occurring in the UAV during flight, the GS-PID controller will switch the controller gains under normal flight conditions to the pre-tuned and fault-related gains to handle the faults during the flight of the UAV.

During recent years, Unmanned Aerial Vehicles (UAVs) have proved to hold a significant role in the world of aviation. These UAVs also provide the academic and industrial researchers and developers feasible and lost-cost test-beds for fault-tolerant control techniques development and flight testing verification (Jordan, et al, 2006; Jourdan et al, 2010; Gregory, Gadiant, & Lavretsky, 2011), which was

extremely difficult and costly by using manned aircraft, since flight testing verification with UAVs does not involve the main concern and the burden for flight testing the developed fault-tolerant control algorithms with human pilot sitting on the manned aircraft/aerial vehicles. These facts motivated also us for building and testing our developed fault-tolerant control algorithms with UAVs through financial supports of NSERC (Natural Sciences and Engineering Research Council of Canada) through a Strategic Project Grant (SPG) and a Discovery Project Grant (DPG) since 2007 leading by the third author. With consideration of an UAV with both in-door and out-door flying capability, a rotorcraft-type UAV, instead of a fixed-wing UAV as developed in the above-mentioned NASA (National Aeronautics and Space Administration) and DRAPA (Defense Advanced Research Projects Agency) sponsored projects in USA (Jordan, et al, 2006; Jourdan et al, 2010), was selected for such an UAV test-bed development and flight tests. Among the rotorcrafts, quadrotor helicopters can usually afford a larger payload than conventional helicopters due to their four-rotor configuration. Moreover, small quadrotor helicopters possess a great manoeuvrability and are potentially simpler to manufacture. For these advantages, quadrotor helicopters have received much and continuously increasing interest in UAV research, development, and applications. The quadrotor helicopter we consider in this work is an under-actuated system with six outputs and four inputs and the states are highly coupled. There are four fixed-pitch-angle blades whereas single-rotor helicopters have variable-pitch-angle (collective) blades.

Control of a quadrotor helicopter UAV is performed by varying the speed of each rotor. The configuration, structure, and related hardware/software of a quadrotor, especially the Quanser quadrotor unmanned helicopter, called as Qball-X4, which is used as the test-bed of this paper's work and was developed in collaboration between Concordia University and Quanser Inc. through an NSERC Strategic Project Grant (SPG), will be presented in the Section 2 of this paper. Nonlinear and linearized state-space models are presented in Section 3 for the purpose of controller design with MRAC. Descriptions of the GS-PID and MRAC with applications to the Qball-X4 are presented in Section 4 and Section 5, respectively. Experimental flight testing results and comparison between GS-PID and MRAC are presented in Section 6. The conclusion and our future work are outlined in Section 7.

2. GENERAL AND QBALL-X4 QUADROTOR HELICOPTER STRUCTURE

In Fig. 1, the conceptual demonstration of a quadrotor helicopter is shown. Each rotor produces a lift force and moment. The two pairs of rotors, i.e., rotors (1, 3) and rotors (2, 4) rotate in opposite directions so as to cancel the

moment produced by the other pair. To make a roll angle (ϕ) along the x -axis of the body frame, one can increase the angular velocity of rotor (2) and decrease the angular velocity of rotor (4) while keeping the whole thrust constant. Likewise, the angular velocity of rotor (3) is increased and the angular velocity of rotor (1) is decreased to produce a pitch angle (θ) along the y -axis of the body frame. In order to perform yawing motion (ψ) along the z -axis of the body frame, the speed of rotors (1, 3) is increased and the speed of rotors (2, 4) is decreased.

The quadrotor helicopter is assumed to be symmetric with respect to the x and y axes so that the center of gravity is located at the center of the quadrotor and each rotor is located at the end of bars.

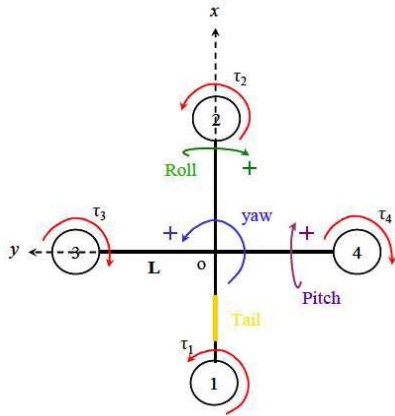


Figure 1. Quadrotor helicopter configuration with Roll-Pitch-Yaw Euler angles [ϕ , θ , ψ]

The quadrotor made by Quanser, known as Qball-X4 as shown in Fig. 2, is an innovative rotary-wing aerial vehicle platform suitable for a wide variety of UAV research and development applications. The Qball-X4 is a quadrotor helicopter propelled by four motors fitted with 10-inch propellers. The entire quadrotor is enclosed within a protective carbon fibre cage for the safety concern during flight to the quadrotor itself and for personnel using it in an in-door environment with limited flying space.

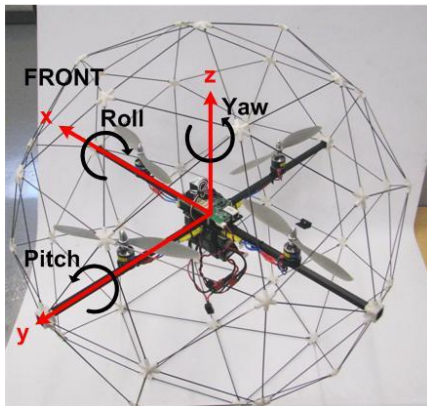


Figure 2. The Qball-X4 quadrotor UAV (Quanser, 2010)

The Qball-X4's proprietary design ensures safe operation as well as opens the possibilities for a variety of novel applications. The protective cage is a crucial feature since this unmanned aerial vehicle was designed for use in an indoor environment/laboratory, where there are typically many close-range hazards (including other vehicles) and personnel doing flight tests with the Qball-X4. The cage gives the Qball-X4 a decisive advantage over other vehicles that would suffer significant damage if contact occurs between the vehicle and an obstacle. To obtain the measurement from on-board sensors and to drive the motors connected to the four propellers, the Qball-X4 utilizes Quanser's onboard avionics Data Acquisition Card (DAQ), the HiQ, and the embedded Gumstix computer. The HiQ DAQ is a high-resolution Inertial Measurement Unit (IMU) and avionics Input/Output (I/O) card designed to accommodate a wide variety of research applications. QuaRC, Quanser's real-time control software, allows researchers and developers to rapidly develop and test controllers on actual hardware through a MATLAB/Simulink interface. QuaRC's open-architecture hardware and extensive Simulink blockset provides users with powerful control development tools. QuaRC can target the Gumstix embedded computer automatically to generate code and execute controllers on-board the vehicle. During flights, while the controller is executing on the Gumstix, users can tune parameters in real-time and observe sensor measurements from a host ground station computer (PC or laptop) (Quanser, 2010).

The interface to the Qball-X4 is MATLAB/Simulink with QuaRC. The controllers are developed in Simulink with QuaRC on the host computer, and these models are downloaded and compiled into executable codes on the target (Gumstix) seamlessly. A diagram of this configuration is shown in Figure 3.

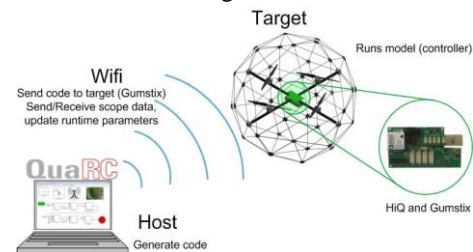


Figure 3. The Qball-X4 communication hierarchy and communication diagram (Quanser, 2010)

For Qball-X4, the following hardware and software are embedded:

- **Qball-X4:** as shown in the Figure 2.
- **HiQ:** QuaRC aerial vehicle data acquisition card (DAQ).
- **Gumstix:** The QuaRC target computer. An embedded, Linux-based system with QuaRC runtime software installed.
- **Batteries:** Two 3-cell, 2500 mAh Lithium-Polymer batteries.

- **Real-Time Control Software:** The QuaRC-Simulink configuration, as detailed in Quanser (2010).

3. MODELING OF THE QBALL-X4

3.1 Non-linear Model of the Qball-X4

In Qball-X4, there are four (E-flite Park 400) brushless motors, using a 10×4.7 inch propeller. As explained before, in order to cancel the moment of each pair of propellers, the motors 1 and 2 have clockwise rotation and the motors 3 and 4 have counterclockwise rotation.

For every attitude change the angular velocity of motors is changed, but the total thrust of all the four motors is constant in order to maintain the height. For instant, to make a pitch angle (θ) along the Y-axis of the body frame one can increase the angular velocity of motor (2) and increase the angular velocity of motor (1), while keeping the trust constant. Likewise the angular velocity of motor (3) is increased and the angular velocity of motor (4) is decreased in order to make a roll angle (ϕ) along the X-axis of the body frame.

It can be understood easily that yaw motion along the Z-axis of the body frame will be implemented by increasing total angular velocity of motors (1, 2) and decreasing the angular velocity of opposite rotation motors (3, 4). Motors of Qball-X4 are not exactly located at the end of the aluminum rods, but 6 inches from the end point for not to touch the fiber carbon cage by propellers and the L is the length between the rotational axis of each motor/rotor and the center of gravity (CoG) of the Qball-X4, as shown in Fig. 4.

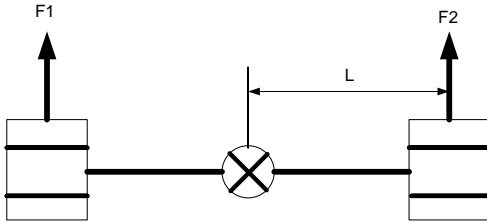


Figure 4. Roll/Pitch axis model

While flying there are four downwash thrust vectors generated by four propellers, if we neglect the drag of four propellers we can present the equations of motion of the Qball-X4 as follows:

$$\begin{bmatrix} \ddot{x} \\ \ddot{y} \\ \ddot{z} \end{bmatrix} = \frac{1}{m} \left(\sum_{i=1}^4 F_i \right) \text{Re}_3 + (g_r(z) - g) e_3 \quad (1)$$

$$\begin{aligned} \ddot{\phi} &= l(F_3 - F_4) / J_1 \\ \ddot{\theta} &= l(F_1 - F_2) / J_2 \\ \ddot{\psi} &= \rho(F_1 + F_2 - F_3 - F_4) / J_3 \end{aligned} \quad (2)$$

where J is the moment of inertia with respect to each axis and ρ is the force-to-moment scaling factor; $[x, y, z]$ are the position of the quadrotor in earth position and $[\phi, \theta, \Psi]$ are roll, pitch and yaw angle respectively.

As mentioned before, we need a transformation matrix which transforms variables from body frame to the Earth frame. Therefore, R represents the coordinate transformation matrix from body frame to earth frame and $e_3 = [0, 0, 1]^T$.

$$R = \begin{bmatrix} \cos \theta \cos \psi & \sin \phi \sin \theta \cos \psi - \cos \phi \sin \psi & \cos \phi \sin \theta \cos \psi + \sin \phi \sin \psi \\ \cos \theta \sin \psi & \sin \phi \sin \theta \sin \psi + \cos \phi \cos \psi & \cos \phi \sin \theta \sin \psi - \sin \phi \cos \psi \\ -\sin \theta & \sin \phi \cos \theta & \cos \phi \cos \theta \end{bmatrix} \quad (3)$$

We can assume that a certain height of the quadrotor, certain ground effects will affect Qball-X4 and we define $g_r(z)$ for such an effect as follows:

$$g_r(z) = \begin{cases} \frac{A}{(z + z_{cg})^2} - \frac{A}{(z_0 + z_{cg})^2} & 0 < z \leq z_0 \\ 0 & \text{else} \end{cases} \quad (4)$$

In this equation we consider A as ground effects and z_{cg} is the Z component of CoG. Because it is very difficult to derive the exact equations for the ground effects, the term $g_r(z)$ is considered as an unknown perturbation in control design, which requires compensation or adaptation. We can simplify (1) and (2), by defining input terms as in (5). u_1 represents the normalized total lift force, and u_2 , u_3 and u_4 correspond to the control inputs of roll, pitch and yaw moments, respectively.

$$\begin{aligned} u_1 &= (F_1 + F_2 + F_3 + F_4) / m \\ u_2 &= (F_3 - F_4) / J_1 \\ u_3 &= (F_1 - F_2) / J_2 \\ u_4 &= \rho(-F_1 - F_2 + F_3 + F_4) \end{aligned} \quad (5)$$

Then the equation of motion can be re-written as below:

$$\ddot{x} = u_1 (\cos \phi \sin \theta \cos \psi + \sin \phi \sin \psi) \quad (6)$$

$$\ddot{y} = u_1 (\cos \phi \sin \theta \sin \psi - \sin \phi \cos \psi) \quad (7)$$

$$\ddot{z} = u_1 (\cos \phi \cos \theta) - g + g_r(z) \quad (8)$$

$$\ddot{\phi} = u_2 l \quad (9)$$

$$\ddot{\theta} = u_3 l \quad (10)$$

$$\ddot{\psi} = u_4 \quad (11)$$

By defining state and input vectors as $\mathbf{x} = [x, y, z, \phi, \theta, \psi]$ and $\mathbf{u} = [u_1, u_2, u_3, u_4]$, the matrix-vector form of the above equations of motion can be represented as:

$$\ddot{\mathbf{x}} = \mathbf{f}(\mathbf{x}) + \mathbf{g}(\mathbf{x})\mathbf{u} + \mathbf{f}_r(\mathbf{x}), \quad (12)$$

where

$$\mathbf{f}(\mathbf{x}) = \begin{bmatrix} 0 \\ 0 \\ -g \\ 0 \\ 0 \\ 0 \end{bmatrix}, \quad \mathbf{f}_r(\mathbf{x}) = \begin{bmatrix} 0 \\ 0 \\ g_r(z) \\ 0 \\ 0 \\ 0 \end{bmatrix}, \quad (13)$$

and $\mathbf{g}(\mathbf{x})$ is defined as follows:

$$\mathbf{g}(\mathbf{x}) = \begin{bmatrix} \cos \phi \sin \theta \cos \psi + \sin \phi \sin \psi & 0 & 0 & 0 \\ \cos \phi \sin \theta \sin \psi - \sin \phi \cos \psi & 0 & 0 & 0 \\ \cos \phi \cos \theta & 0 & 0 & 0 \\ 0 & l & 0 & 0 \\ 0 & 0 & l & 0 \\ 0 & 0 & 0 & 1 \end{bmatrix} \quad (14)$$

3.2 Linearized State-Space Model of the Qball-X4

This section describes the linearized dynamic model of the Qball-X4 for the purpose of designing linear controller, such as MRAC. For the following discussion, the axes of the Qball-X4 are denoted as (x, y, z) and defined with respect to the configuration of the Qball-X4 as shown in Figure 2. Roll, pitch, and yaw are defined as the angles of rotation about the x , y , and z axis, respectively. The global workspace axes are denoted as (X, Y, Z) and defined with the same orientation as the Qball-X4 sitting upright on the ground.

Actuator Dynamics

To count into dynamics of the actuators in Qball-X4 modeling, the thrust generated by each propeller is modeled using the following first-order system:

$$\mathbf{F} = k \frac{\omega}{s + \omega} \mathbf{u} \quad (15)$$

where u is the PWM input to the DC-motor actuator, ω is the actuator bandwidth and K is a positive gain. These parameters were calculated and verified through experimental studies. A state variable, v , will be used to represent the actuator dynamics, which is defined as follows:

$$v = \frac{\omega}{s + \omega} u \quad (16)$$

Roll and Pitch Models

Assuming that rotations about the x and y axes are decoupled, the motion in roll/pitch axis can be modeled as shown in Figure 4. As illustrated in the figure, two propellers contribute to the motion in each axis. The thrust generated by each motor can be calculated from Eq. (15) and used as corresponding input. The rotation around the center of gravity is produced by the difference in the generated thrusts. The roll/pitch angle can be formulated using the following dynamics:

$$J \ddot{\theta} = \Delta FL \quad (17)$$

where

$$J = J_{roll} = J_{pitch} \quad (18)$$

are the rotational inertia of the device in roll and pitch axes. L is the distance between the propellers and the center of gravity, and

$$\Delta F = F1 - F2 \quad (19)$$

represents the difference between the forces generated by the propeller pair (1, 2).

By combining the dynamics of motion for the roll/pitch axis and the actuator dynamics for each propeller the following state-space equations can be derived:

$$\begin{bmatrix} \dot{\theta} \\ \ddot{\theta} \\ \dot{v} \end{bmatrix} = \begin{bmatrix} 0 & 1 & 0 \\ 0 & 0 & \frac{KL}{J} \\ 0 & 0 & -\omega \end{bmatrix} \begin{bmatrix} \theta \\ \dot{\theta} \\ v \end{bmatrix} + \begin{bmatrix} 0 \\ 0 \\ \omega \end{bmatrix} \Delta F \quad (20)$$

To facilitate the use of an integrator in the feedback structure a fourth state can be added to the state vector, which is defined as $\dot{s} = \theta$.

Height Model

The motion of the Qball-X4 in the vertical direction (along with the Z axis) is affected by all the four propellers. The dynamic model of the Qball-X4 in this case can be written as:

$$M \ddot{Z} = 4F \cos(r) \cos(p) - Mg \quad (21)$$

where F is the thrust generated by each propeller, M is the total mass of the propeller, Z is the height and r and p represent the roll and pitch angular rates, respectively. As expressed in this equation, if the roll and pitch angular rates are nonzero the overall thrust vector will not be perpendicular to the ground. Assuming that roll and pitch angles are close to zero, the dynamic equations can be linearized to the following state space form:

$$\begin{bmatrix} \dot{z} \\ \ddot{z} \\ \dot{v} \\ \dot{s} \end{bmatrix} = \begin{bmatrix} 0 & 1 & 0 & 0 \\ 0 & 0 & \frac{4K}{M} & 0 \\ 0 & 0 & -\omega & 0 \\ 1 & 0 & 0 & 0 \end{bmatrix} \begin{bmatrix} z \\ \dot{z} \\ v \\ s \end{bmatrix} + \begin{bmatrix} 0 \\ 0 \\ \omega \\ 0 \end{bmatrix} u + \begin{bmatrix} 0 \\ 0 \\ 0 \\ -g \end{bmatrix} \quad (22)$$

X-Y Position Model

The motions of the Qball-X4 along the X and Y axes are caused by the total thrust and by changes of the roll/pitch angles. Assuming that the yaw angle is zero, the dynamics of motion in X and Y axes can be written as:

$$\begin{aligned} M\ddot{X} &= 4F \sin(p) \\ M\ddot{Y} &= -4F \sin(r) \end{aligned} \quad (23)$$

Assuming that the roll and pitch angle rates are close to zero, the following linear state-space equations can be derived for X and Y positions.

$$\begin{bmatrix} \dot{X} \\ \ddot{X} \\ \dot{v} \\ \dot{s} \end{bmatrix} = \begin{bmatrix} 0 & 1 & 0 & 0 \\ 0 & 0 & \frac{4K}{M} & 0 \\ 0 & 0 & -\omega & 0 \\ 1 & 0 & 0 & 0 \end{bmatrix} \begin{bmatrix} X \\ \dot{X} \\ v \\ s \end{bmatrix} + \begin{bmatrix} 0 \\ 0 \\ \omega \\ 0 \end{bmatrix} u \quad (24)$$

$$\begin{bmatrix} \dot{Y} \\ \ddot{Y} \\ \dot{v} \\ \dot{s} \end{bmatrix} = \begin{bmatrix} 0 & 1 & 0 & 0 \\ 0 & 0 & -\frac{4K}{M} & 0 \\ 0 & 0 & -\omega & 0 \\ 1 & 0 & 0 & 0 \end{bmatrix} \begin{bmatrix} Y \\ \dot{Y} \\ v \\ s \end{bmatrix} + \begin{bmatrix} 0 \\ 0 \\ \omega \\ 0 \end{bmatrix} u \quad (25)$$

Yaw Model

The torque generated by each motor, τ , is assumed to have the following relationship with respect to the PWM input, u

$$\tau = K_y u \quad (26)$$

where K_y is a positive gain. The motion in the yaw axis is caused by the difference between the torques exerted by the two clockwise and the two counterclockwise rotating props. The motion in the yaw axis can be modeled by:

$$J_y \ddot{\theta}_y = \Delta \tau \quad (27)$$

where θ_y is the yaw angle and J_y is the rotational inertia about the z axis. The resultant torque of the motors, $\Delta \tau$, can be calculated by:

$$\Delta \tau_y = -\tau_1 - \tau_2 + \tau_3 + \tau_4 \quad (28)$$

The yaw axis dynamics can be rewritten in the state-space form as:

$$\begin{bmatrix} \dot{\theta}_y \\ \ddot{\theta}_y \end{bmatrix} = \begin{bmatrix} 0 & 1 \\ 0 & 0 \end{bmatrix} \begin{bmatrix} \theta_y \\ \dot{\theta}_y \end{bmatrix} + \begin{bmatrix} 0 \\ \frac{K_y}{J_y} \end{bmatrix} \Delta \tau_y \quad (29)$$

4. GAIN-SCHEDULED PROPORTIONAL-DERIVATIVE-INTEGRAL (GS-PID) CONTROLLER

In view of the advantages of widely used Proportional-Integral-Derivative (PID) controller and gain scheduling control strategy in aerospace and industrial applications, a control strategy by using gain scheduling based PID controller is proposed for fault tolerant control (FTC) of our UAV test-bed Qball-X4.

As described previously, PID controllers are designed and tuned in both fault-free and faulty situations to control the Qball-X4 under normal and faulty flight conditions.

For GS-PID controller, several sets of pre-tuned gains are applied to the controllers in different flight conditions under both fault-free and faulty cases. In the next step, attempts to obtain the best stability and performance of Qball-X4 in trajectory tracking control under both cases and to switch the controller gains from one set of pre-tuned PID controller to another set of the gains in the presence of different levels of actuator faults are carried out.

One of the main parameters to consider in GS-PID is the switching time between the time of fault occurrence and the time of switching to new set of gains. In other words, if this transient (switching) time is held long (more than one second) it can cause the Qball-X4 to hit the ground and cause a crash, since the operating height was considered as 70 cm to 1 meter. The structure of a GS-PID controller implemented in the Qball-X4 software environment is shown in Figure 5.

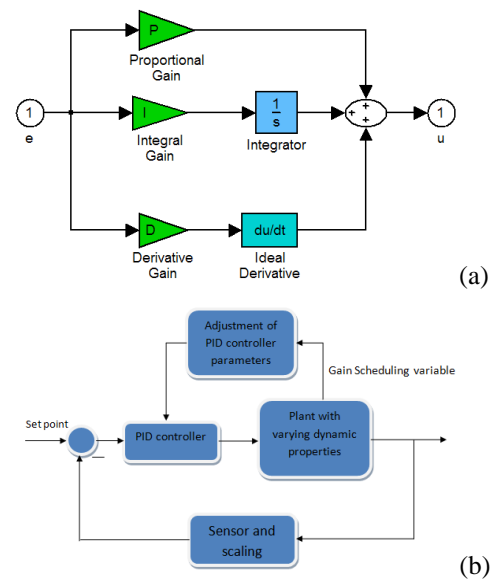


Figure 5. (a) PID and (b) GS-PID controller structures

5. MODEL REFERENCE ADAPTIVE FAULT/DAMAGE TOLERANT CONTROLLER

Model Reference Adaptive Control (MRAC) is concerned with forcing the dynamic response of the controlled system to asymptotically approach that of a reference system, despite parametric uncertainties (faults) in the system. Two major subcategories of MRAC are those of *indirect methods*, in which the uncertain plant parameters are estimated and the controller redesigned online based on the estimated parameters, and *direct methods*, in which the tracking error is forced to zero without regard to parameter estimation accuracy (though under certain conditions related to the level of excitation in the command signal, the adaptive laws often can converge to the proper values). MRAC for linear systems has received, and continues to receive, considerable attention in the literature. Based on the advantages of the direct method without the need of estimation of unknown parameters for implementing the adaptive controller as required by the indirect method, direct method is selected in this work for fault-tolerant control of the Qball-X4. The control structure of such a MRAC scheme can be represented as in Fig. 6.

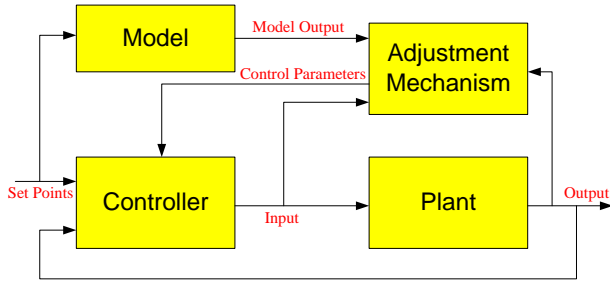


Figure 6. Model reference adaptive control structure

There are different approaches to MRAC design, such as:

- The MIT rule
- Lyapunov stability theory
- Hyperstability and passivity theory
- The error model
- Augmented error
- Model-following MRAC
- Modified-MRAC (M-MRAC)
- Conventional MRAC (C-MRAC)

In this paper, the MIT rule is used to design the MRAC for the height hold and trajectory tracking of the Qball-X4. However, the schemes based on the MIT rule and other approximations may go unstable. We illustrate the use of the MIT rule for the design of an MRAC scheme for the plant

$$\ddot{y} = -a_1\dot{y} - a_2y + u \quad (30)$$

where a_1 and a_2 are the unknown plant parameters, and \dot{y} and y are available for measurement. The reference model to be matched by the closed-loop plant is given by:

$$\ddot{y}_m = -2\dot{y}_m - y_m + r \quad (31)$$

The control law is then given by:

$$u = \theta_1^*\dot{y} + \theta_2^*y + r \quad (32)$$

where

$$\theta_1^* = a_1 - 2, \theta_2^* = a_2 - 1 \quad (33)$$

will achieve perfect model following. The equation (33) is referred to as the matching equation. Because a_1 and a_2 are unknown, the desired values of the controller parameters θ_1^* and θ_2^* cannot be calculated from (33). Therefore, following control law are used instead:

$$u = \theta_1\dot{y} + \theta_2y + r \quad (34)$$

where θ_1 and θ_2 are adjusted using the MIT rule as:

$$\dot{\theta}_1 = -\gamma e_1 \frac{\partial y}{\partial \theta_1}, \dot{\theta}_2 = -\gamma e_2 \frac{\partial y}{\partial \theta_2} \quad (35)$$

where $e_1 = y - y_m$. To implement (35), we need to generate the sensitivity functions $\frac{\partial y}{\partial \theta_1}, \frac{\partial y}{\partial \theta_2}$ online.

6. EXPERIMENTAL FLIGHT TESTING RESULTS

6.1 Flight Testing Results with GS-PID

For comparison purpose and as a baseline controller of the Qball-X4 under normal flight conditions, a single PID controller, which is tuned well for taking-off, hovering and landing scenario under normal flight condition is designed first. Such a controller is used also in a faulty scenario with an 18% of overall loss in power of all motors. Since the significantly deteriorated performance by using a single PID controller, in particular when the fault level increases, another set of PID gains is set for the fault case with gain scheduling strategy for a better handling of the fault comparing with a single PID controller mainly designed and turned for normal flight of the Qball-X4. To analyze the effect of time delay due to fault detection and diagnosis scheme, different levels of time delay were introduced when scheduling/switching the controller gains after a fault occurrence since such fault detection induced time delay is essential for maintaining the stability and the acceptable performance of the Qball-X4 after fault occurrence.

Flight tests with a one meter circuit leg square trajectory tracking scenario for cases with different time delays have been carried out. As shown in Fig. 7, acceptable tracking deviation from the desired square trajectory after the fault occurrence can be obtained with the case of 0.5 sec time delay. Better tracking performance with a shorter time delay can be achieved which verified the importance of fast and correct fault detection and control switching (reconfiguration) after fault occurrence.

To demonstrate the possible best performance without time delay, i.e. the fault occurrence and the switching of controller gains occur at the same time with the perfect fault detection and isolation, the best result can be achieved by the GS-PID is shown in Fig. 8 where the fault occurred and the PID controller is switched at the same time of 20s. Better tracking performance has been achieved compared to the case with 0.5 s time delay as shown in Fig. 7. Videos on the above flight testing results are available at <http://users.encs.concordia.ca/~ymzhang/UAVs.htm>.

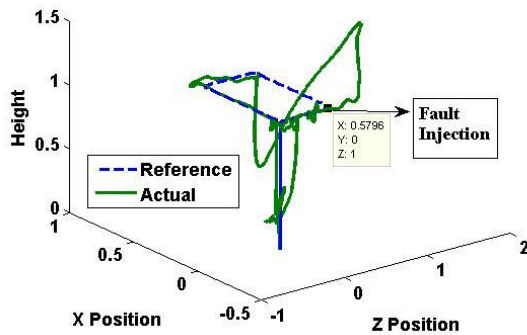


Figure 7. GS-PID with a time delay of 0.5 sec for controller switching in the presence of an actuator fault

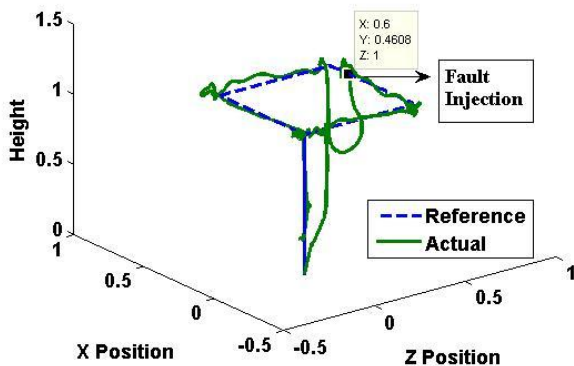


Figure 8. GS-PID without time delay for controller switching in faulty condition (the best performance can be achieved with the designed GS-PID)

6.2 Flight Testing Results with MRAC

Regarding MRAC, hovering control as well as square trajectory tracking controls with fault injection are applied to Qball-X4 and the experimental flight testing results are shown in Figs. 9 and 10. In Fig. 9, a fault-free condition is applied to the Qball-X4 and the MRAC was able to track the trajectory close to real one. In Fig. 10, a fault is injected to the left and back motors at 20 sec with a loss of 18% of power during the flight. As can be seen from Fig. 10, Qball-X4 can still track the desired trajectory with a safe landing. Relevant flight testing videos are also available at <http://users.encs.concordia.ca/~ymzhang/UAVs.htm>.

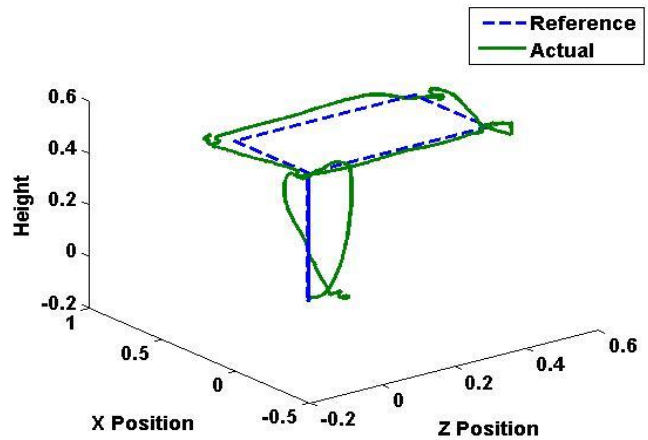


Figure 9. Square trajectory in fault-free condition with MRAC

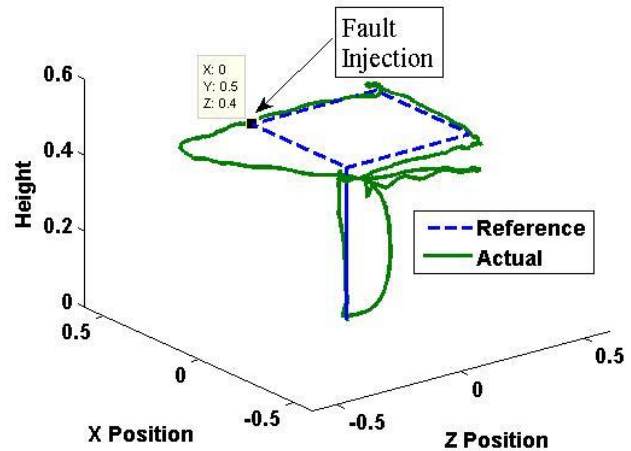


Figure 10. Square trajectory in faulty condition (left and back motors) with MRAC

6.3 Comparison and Comments Based on This Research

During this research many hours of flight tests have been spent at the Network Autonomous Vehicle Laboratory

(NAVL) of the Mechanical and Industrial Department at Concordia University in order to develop the GS-PID and MRAC for achieving the best fault-tolerant control performance of the Qball-X4 under fault flight conditions. By our experience and comparison of the flight testing results, it can be concluded that the MRAC yields a better response than GS-PID for trajectory tracking control although the GS-PID is easier to design and to implement in MATLAB/Simulink interface of the Qball-X4 as well as in the simulation environment. In fact, the GS-PID can give a better result if the tuning for controller gains at pre-fault and faulty cases be very precise. A good tuning for the GS-PID controller gains was very time consuming and gains could change from one flight to another even in our in-door lab environment. Any change in lab environment during flight could force the gains need to be tuned again. However, the MRAC is more reliable and robust to the lab noises and environment changes. Together with the advantages without the need of mathematical model in GS-PID design and implementation compared with MRAC (where a mathematical model is needed to design and implement the controller), GS-PID control technique can play an important role for fault-tolerant control of UAVs as the same as its wide and successful applications in normal/fault-free cases, with the support of an effective and efficient automatic control gains tuning techniques.

7. CONCLUSION AND FUTURE WORK

In this paper, two types of popular controllers, Proportional-Integral-Derivative (PID) controller with Gain Scheduling (GS) technique and Model Reference Adaptive Control (MRAC), are applied and tested, in a quadrotor helicopter UAV test-bed and the results are presented. Both controllers showed good results for height control of the quadrotor UAV: Qball-X4. Unlike the GS-PID, the single PID which is tuned for normal flight was not able to handle the faults with larger fault level.

The future work is considered to combine the GS-PID fault-tolerant control with an online fault detection and diagnosis scheme to achieve an entire active fault-tolerant GS-PID control of the Qball-X4 and other UAVs. Investigation and implementation of efficient auto-tuning strategies for GS-PID is also an important future work although these GS-PID controller gains do not need to be designed on-line in real-time.

REFERENCES

- A. Bani Milhim, Y. M. Zhang, and C.-A. Rabbath, "Gain Scheduling Based PID Controller for Fault Tolerant Control of a Quad-Rotor UAV," *AIAA Infotech@Aerospace 2010*, 20-22 April 2010, Atlanta, Georgia, USA.
- B. T. Whitehead, S. R. Bieniawski, "Model Reference Adaptive Control of a Quadrotor UAV," *AIAA Guidance, Navigation, and Control Conference*, 2-5 August 2010, Toronto, Ontario, Canada.
- D. Jourdan et al, "Enhancing UAV Survivability Through Damage Tolerant Control," *AIAA Guidance, Navigation, and Control Conference*, Toronto, Ontario, Canada, 2-5 Aug. 2010.
- E. N. Johnson, G. V. Chowdhary, and M. S. Kimbrell, "Guidance and Control of an Airplane under Severe Structural Damage," *AIAA Infotech@Aerospace 2010*, 20-22 April 2010, Atlanta, Georgia, USA.
- I. Gregory, R. Gadiant, and E. Lavretsky, "Flight Test of Composite Model Reference Adaptive Control (CMRAC) Augmentation Using NASA AirSTAR Infrastructure," *AIAA Guidance, Navigation, and Control Conference*, 8-11 August 2011, Portland, Oregon, USA.
- J. Guo and G. Tao, "A Multivariable MRAC Scheme Applied to the NASA GTM with Damage," *AIAA Guidance, Navigation, and Control Conference*, 2-5 August 2010, Toronto, Ontario, Canada.
- J. Levin, "Alternative Model Reference Adaptive Control," *AIAA Guidance, Navigation, and Control Conference*, 2-5 August 2010, Toronto, Ontario, Canada.
- K. A. Lemon, J. E. Steck, and B. T. Hinson, "Model Reference Adaptive Flight Control Adapted for General Aviation: Controller Gain Simulation and Preliminary Flight Testing on a Bonanza Fly-By-Wire Testbed," *AIAA Guidance, Navigation, and Control Conference*, 2-5 August 2010, Toronto, Ontario, Canada.
- L. G. Crespo, M. Matsutani and A. M. Annaswamy, "Design of a Model Reference Adaptive Controller for an Unmanned Air Vehicle," *AIAA Guidance, Navigation, and Control Conference*, 2-5 August 2010, Toronto, Ontario, Canada.
- Quanser Inc., Qball User Manual, available at http://www.quanser.com/english/html/UVS_Lab/fs_Qball_X4.htm
- R. Gadiant, J. Levin, and E. Lavretsky, "Comparison of Model Reference Adaptive Controller Designs Applied to the NASA Generic Transport Model," *AIAA Guidance, Navigation, and Control Conference*, 2-5 August 2010, Toronto, Ontario, Canada.
- T. Bierling, L. Hocht and F. Holzapfel, "Comparative Analysis of MRAC Architectures in a Unified Framework," *AIAA Guidance, Navigation, and Control Conference*, 2-5 August 2010, Toronto, Ontario, Canada.
- T. L. Jordan, J. V. Foster, R. M. Bailey, and C. M. Belcastro, "AirSTAR: A UAV Platform for Flight Dynamics and Control System Testing," *AIAA Aerodynamic Measurement Technology and Ground Testing Conference*, San Francisco, CA, 2006.

- V. Stepanyan, S. Campbell, and K. Krishnakumar, "Adaptive Control of a Damaged Transport Aircraft Using M-MRAC," *AIAA Guidance, Navigation, and Control Conference*, 2-5 August 2010, Toronto, Ontario, Canada.
- Y. M. Zhang and J. Jiang, "Bibliographical Review on Reconfigurable Fault-tolerant Control Systems," *Annual Reviews in Control*, 32(2), 2008, pp. 229-252.
- Z. T. Dydek and A. M. Annaswamy, "Combined/Composite Adaptive Control of Quadrotor UAV in the Presence of Actuator Uncertainty," *AIAA Guidance, Navigation, and Control Conference*, 2-5 August 2010, Toronto, Ontario, Canada.